Article

Hydrodynamic forces exerted on an oscillating cylinder at its translational motion in water covered by a compressed ice

Yury Stepanyants [1,2,*] and Izolda Sturova [3]

1 School of Sciences, University of Southern Queensland, QLD 4350, Australia
2 Department of Applied Mathematics, Nizhny Novgorod State Technical University, Nizhny Novgorod, 603950, Russia; Yury.Stepanyants@usq.edu.au
3 Lavrentyev Institute of Hydrodynamics of Siberian Branch of Russian Academy of Sciences, Novosibirsk, 630090, Russia; Sturova@hydro.nsc.ru
* Correspondence: Yury.Stepanyants@usq.edu.au

Abstract: We calculate the hydrodynamic forces exerted on an oscillating circular cylinder when it moves translationally perpendicular to its axis in the infinitely deep water covered by compressed ice. The cylinder can oscillate both horizontally and vertically. In the linear approximation, we find a solution for the steady wave motion generated by the cylinder within the hydrodynamic set of equations for the incompressible ideal fluid. We show that depending on the rate of ice compression, the normal and anomalous dispersion can occur in the system. In the latter case, the group velocity can be opposite to the phase velocity in a certain range of wavenumbers. We investigate the dependences of the hydrodynamic loads (added mass, damping coefficients, wave resistance, and lift force) exerting on the cylinder on the translational velocity and frequency of oscillation. It is shown that there is a possibility of the appearance of negative values for the damping coefficients at the relatively big cylinder velocity; then the wave resistance decreases with increasing of cylinder velocity. The theoretical results are underpinned by the numerical calculations for the real parameters of ice and cylinder motion.

Keywords: Ideal fluid; deep water; ice cover; moving cylinder; hydrodynamic load; added mass; wave resistance; damping coefficient

1. Introduction

As well known, a significant proportion of World oil and gas reserves (up to 80% percent according to some estimates) are concentrated on the shelf of the surrounding oceans and seas. In recent years, the volume of hydrocarbon production in the shelf zone has been growing rapidly; this stimulates the rapid growth of onshore and offshore engineering construction. In many countries, offshore projects are intensively developing. One of the priority areas for the development of the energy sector is the exploration of the Arctic and, possibly, Antarctic oil and gas fields. Progress in the development of natural resources of the sea shelf is inextricably linked with the study of hydrodynamic processes on the shelf and the ability to effectively describe and predict them. This is especially important in relation to the study of extreme events. Due to the specifics of the circumpolar regions, the development of research in the oceans and seas covered with ice is of great importance. Large sea areas where research, energy production or the construction of hydraulic structures (platforms, oil and gas pipelines) are conducted, may be covered with pack ice, broken ice, or solid ice, which is in a stress state due to wind influences or pressure from outside mainland ice. According to available data, up to 12% of the oceans and seas are covered with ice. Most of the ice cover is found in the circumpolar regions, but during particularly cold winters the ice cover can deviate significantly south in the Northern Hemisphere or north in the Southern Hemisphere.

In many cases, there are currents in the ocean beneath the ice cover. The currents can cause vibrations of pipelines leading to the wave motion in the ice. At certain conditions, the instability can arise resulting in the simultaneous growth of pipeline oscillations and flexural-gravity wave (FGW) amplitude in the ice cover. Therefore, the problem of description of such a phenomenon is topical and important from the practical point of view. It is also important to calculate the hydrodynamic loads exerting on the pipelines in the current in the seas or oceans covered by ice.

Quite a lot of works have been devoted to the problem of studying waves in an ocean with an ice cover, among which the pioneering publications dating back to the 1960s can be mentioned [9,10]. Since that time, joint systems of equations describing wave disturbances in water and in an infinite homogeneous ice plate have been studied by many authors (see, for example, the reviews [15,20,25] and references therein). In addition, FGWs in the ice cover generated by underwater sources were studied for both stationary and moving fluid of finite or infinite depth [6,8,14,16–19]. Effective direct mathematical methods for studying wave interactions with floating flexible structures have been developed by many authors and are described in the book by Sahoo [15].

Under natural conditions, an ice sheet on water can undergo compression or tension due to wind stress and pressure from other ice areas, for example, due to the sliding of continental ice into the ocean. This makes it relevant to study FGWs in oceans covered with compressed ice. This problem becomes very nontrivial from the theoretical point of view, since it leads to a wide variety of possible cases due to a rather complex dispersion relation for this type of waves (see, for example, [3–5,21]. In the recently published work by the current authors [21], FGWs generated by a dipole moving horizontally at some depth under the ice and oscillating along the direction of motion were studied. Neglecting the effects of viscosity in water and in an ice plate, the basic equations of wave motion for a fluid of finite depth were derived. The wave patterns generated by a cylinder of finite radius in an infinitely deep ocean were also analyzed in detail. The added mass coefficients and the damping coefficients acting on the cylinder were found. In the same work, it was shown that the wave motion created by a cylinder of finite radius can be modeled with the reasonable accuracy by the motion of a point dipole. The problem studied represents a particular case of the well-known general problem when in the process of translational motion of a body oscillating along and perpendicular to the motion, the body experiences action of radiative hydrodynamic forces. This problem has been thoroughly investigated in the linear approximation for a submerged cylindrical body moving under a free surface in a homogeneous or two-layer fluid (see, for example, [22,23,26,27] and references therein).

In this paper we examine in detail the effect of floating ice cover on the hydrodynamic loads exerting on the translationally moving and oscillating circular cylinder. In the linear approximation, we find a solution for the steady wave motion generated by the cylinder within the hydrodynamic set of equations for the incompressible ideal fluid of infinite depth. We show that depending on the rate of ice compression, the normal and anomalous dispersion can occur in the system. In the latter case, the group velocity can be opposite to the phase velocity in a certain range of wavenumbers. We investigate the dependences of hydrodynamic loads (the added mass, damping coefficients, wave resistance, and lift force) exerting on the cylinder on the translational velocity and frequency of oscillation. It is shown that there is a possibility of the appearance of negative values for the damping coefficients at the relatively big cylinder velocity; then the wave resistance decreases with increasing of the cylinder velocity. The theoretical results are underpinned by the numerical calculations for the real parameters of ice and cylinder motion.

2. Governing equations and boundary conditions

Let us consider a circular cylinder of a radius a (a pipeline, for example) flowing around by a uniform current with the velocity $\mathbf{U} = -U\nabla x$ in an ideal incompressible fluid of the density ρ (see Figure 1). The cylinder oscillates in the horizontal and vertical directions with the frequency Ω. We assume that the water is infinitely deep containing an ice cover on the top, can be modelled by a thin elastic plate. The main set of hydrodynamic equations and boundary conditions describing FGWs in the linear approximation is as follows. For the velocity potential $\Phi(x, y, t)$ we have the Laplace equation:

$$\Delta\Phi \equiv \frac{\partial^2\Phi}{\partial x^2} + \frac{\partial^2\Phi}{\partial y^2} = 0 \quad (|x| < \infty,\ -\infty < y \leq 0), \tag{1}$$

where the fluid velocity $\mathbf{u} = \nabla\Phi$.

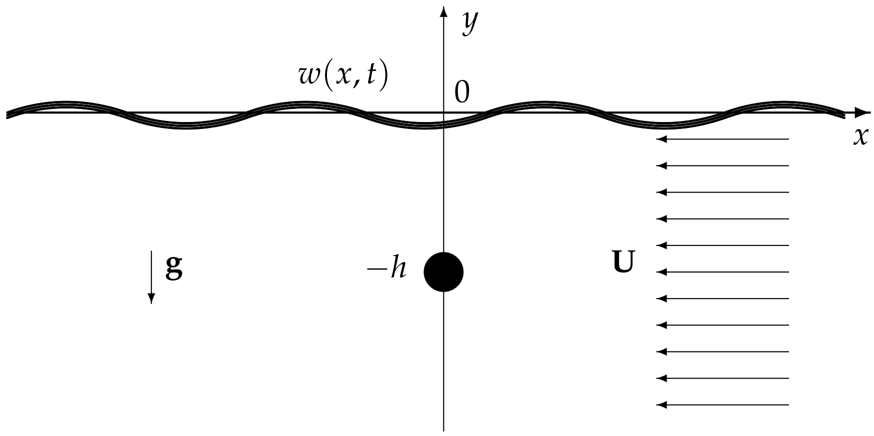

Figure 1. Sketch of the flow around a rigid cylinder in a deep water covered by a flexible ice cover.

It is assumed that the lower boundary of the ice plate is always in contact with the water. By denoting through the $w(x, t)$ the vertical displacements of the ice cover from the undisturbed flat position, the kinematic and dynamic conditions at the upper boundary of the fluid (at $y = 0$) can be written as [21]:

$$\frac{\partial w}{\partial t} - \frac{\partial\Phi}{\partial y} = 0, \tag{2}$$

$$D\frac{\partial^4 w}{\partial x^4} + Q\frac{\partial^2 w}{\partial x^2} + M\frac{\partial^2 w}{\partial t^2} + \rho\, g\, w + \rho\frac{\partial\Phi}{\partial t} = 0, \tag{3}$$

where $D = Eh_1^3/[12(1-\nu^2)]$, $M = \rho_1 h_1$, E is the Young modulus of elastic plate, Q is the longitudinal stress ($Q > 0$ corresponds to compression, and $Q < 0$ – to stretching), other parameters are ν – the Poisson ratio, h_1 – the thickness of the ice plate, g is the acceleration due to gravity. The first term in Eq. (3) describes the elastic property of the ice plate; the second term represents a horizontal stress or strain of the plate; the term with the coefficient M describes the inertial property of the ice plate. All perturbations vanish in the bulk of the fluid so that for the vertical component of fluid velocity we have:

$$\partial\Phi/\partial y \to 0, \quad \text{when} \quad y \to -\infty. \tag{4}$$

The dispersion relation of FGW relating the frequency ω of harmonic waves of infinitesimal amplitude with the wavenumber k is (see, for example, [2,9,21]):

$$\omega(k) = \sqrt{\frac{k(Dk^4 - Qk^2 + \rho\, g)}{\rho + kM}}. \tag{5}$$

The phase and group velocities of FGW are:

$$c_p(k) = \sqrt{\frac{Dk^4 - Qk^2 + \rho\, g}{k(\rho + kM)}}. \tag{6}$$

$$c_g(k) = \frac{2k^3M(2Dk^2 - Q) + \rho\,(5Dk^4 - 3Qk^2 + \rho\, g)}{2\omega(k)(\rho + kM)^2}. \tag{7}$$

As well-known, the dispersion relation (5) imposes a restriction on the maximal value of the compression force. The stability of oscillations of a floating ice plate is guaranteed by the condition $Q < Q_* \equiv 2\sqrt{g\rho D}$, whereas at $Q > Q_*$ the buckling occurs – the ice plate shatters (see, for example, [2,9]). There is one more critical value of the parameter Q such that for $Q < Q_0 < Q_*$ the group velocity of FGW is positive for all wavenumbers $k \geq 0$. Such a case when $c_g > 0$ will be called *the normal dispersion* in contrast to the case of *anomalous dispersion* for $Q_0 < Q < Q_*$, which is characterized by the presence of a wavenumber interval within which the group velocity is negative (details can be found in Ref. [21]). Both these critical values Q_* and Q_0, as well as the corresponding wavenumbers k_* and k_0 can be determined from the solution of two simultaneous equations $c_g(k) = 0$ and $dc_g/dk = 0$.

In this paper, we study a steady regime of fluid motion caused by the translationally moving and oscillating cylinder. In this case, the total potential of fluid velocity can be presented in the form:

$$\Phi(x,y,t) = -Ux + U\overline{\varphi}(x,y) + \mathrm{Re}\sum_{j=1}^{2}\eta_j\varphi_j(x,y)e^{i\Omega t}, \tag{8}$$

where $\overline{\varphi}$ is the velocity potential corresponding to the uniform motion of the body with the unit velocity, φ_j $(j = 1,\ 2)$ are the radiation potentials due to the cylinder oscillation in the horizontal $(j = 1)$ and vertical $(j = 2)$ directions, η_j are the amplitudes of cylinder vibrations in these directions. Similarly to Eq. (8), the vertical displacements of the ice plate can be presented as:

$$w(x,t) = \overline{w}(x) + \mathrm{Re}\left[\sum_{j=1}^{2}\eta_j w_j(x)e^{i\Omega t}\right]. \tag{9}$$

The stationary part of the total potential $\overline{\varphi}$ satisfies the Laplace equation in the fluid:

$$\Delta\overline{\varphi} = 0 \quad (|x| < \infty,\ -\infty < y \leq 0) \tag{10}$$

with the boundary conditions at $y = 0$:

$$\frac{\partial\overline{w}}{\partial x} + \frac{\partial\overline{\varphi}}{\partial y} = 0, \tag{11}$$

$$\left(D\frac{\partial^4}{\partial x^4} + Q\frac{\partial^2}{\partial x^2} + MU^2\frac{\partial^2}{\partial x^2} + \rho g\right)\frac{\partial\overline{\varphi}}{\partial y} + \rho U^2\frac{\partial^2\overline{\varphi}}{\partial x^2} = 0. \tag{12}$$

The boundary conditions far from the source are as follows:

$$\frac{\partial\overline{\varphi}}{\partial y} \to 0 \quad (y \to -\infty), \qquad \frac{\partial\overline{\varphi}}{\partial x} \to \psi_\pm \quad (x \to \pm\infty), \tag{13}$$

where functions $\psi_\pm(x,y)$ are equal to zero if the current speed U is less than the minimal phase speed of FGWs. If $U > (c_p)_{min}$, than functions $\psi_\pm(x,y)$ represent wave disturbances oscillating in x when $x \to \pm\infty$.

On the circular contour $S:\ x^2 + (y+h)^2 = a^2$ which represents the surface of the rigid cylinder, the impermeability condition is posted:

$$\frac{\partial\overline{\varphi}}{\partial n} = n_1\ (x, y \in S), \tag{14}$$

where $\mathbf{n} = (n_1, n_2)$ is the inner normal to the contour S, and h is the distance of the cylinder center from the upper boundary of the fluid $(h > a)$.

The components of radiation potentials also satisfy the Laplace equation:

$$\Delta\varphi_j = 0 \quad (|x| < \infty,\ -\infty < y \leq 0) \tag{15}$$

and the boundary conditions at $y = 0$:

$$\Lambda w_j - \frac{\partial\varphi_j}{\partial y} = 0, \tag{16}$$

$$\left(D\frac{\partial^4}{\partial x^4} + Q\frac{\partial^2}{\partial x^2} + M\Lambda^2 + \rho g\right)w_j + \rho\Lambda\varphi_j = 0, \tag{17}$$

where the operator $\Lambda = i\Omega - U\partial/\partial x$.

The boundary condition on the cylinder circular contour is:

$$\frac{\partial\varphi_j}{\partial n} = i\Omega n_j - Um_j\ (x, y \in S), \tag{18}$$

where $(m_1,\ m_2) = \nabla(\partial\overline{\varphi}/\partial n)$.

In the far-field zone when $x \to \pm\infty$ wave perturbations consist of superposition of several periodic waves (the details will be clarified below).

Hydrodynamic forces $\mathbf{F} = (F_1,\ F_2)$ exerting on the cylinder, are determined by integrating the fluid pressure (less the hydrostatic term) $p = -\rho(\partial\Phi/\partial t + |\nabla\Phi|^2/2)$ along the contour S. It is convenient to replace this integral by the sum

$$F_j = F_{sj} + \mathrm{Re}\left(F_{rj}e^{i\Omega t}\right) \quad (j = 1, 2), \tag{19}$$

where F_{sj} are the stationary force components (the wave resistance and lifting force) acting on a body in a stationary uniform flow, whereas F_{rj} are the radiation forces, which are usually written in the matrix form (for more details, see, for example, [13]): $F_{rj} = \eta_1 T_{j1} + \eta_2 T_{j2}$. The quantities T_{jk} $(k = 1,\ 2)$ represent a complex force acting in the j-direction and caused by sinusoidal oscillations of a body with a unit amplitude in the k-direction; they can be represented as $T_{jk} = \Omega^2\mu_{jk} - i\Omega\lambda_{jk}$. The real quantities μ_{jk} and λ_{jk} are known as the added mass and damping coefficients, respectively.

Let us introduce polar coordinates with the origin in the centre of the contour S, $x = r\sin\theta$, $y = r\cos\theta - h$. Then, taking into account that the components of the unit vector normal to the circular cylinder are

$$n_1 = -\sin\theta, \quad n_2 = -\cos\theta, \tag{20}$$

we obtain (see, e.g., [27]):

$$(F_{s1},\ F_{s2}) = \frac{\rho U^2}{2a}\int_0^{2\pi}\left[\frac{\partial(\overline{\varphi} - x)}{\partial\theta}\right]^2(\sin\theta,\ \cos\theta)\,d\theta, \tag{21}$$

$$T_{jk} = \rho a\int_0^{2\pi}\frac{\partial\varphi_j^*}{\partial n}\varphi_k\,d\theta, \tag{22}$$

where symbol * stands for complex conjugate.

In the next sections we present solutions of stationary problem for the potential $\overline{\varphi}$ and non-stationary problem for the radiation potentials φ_j.

3. Solutions of the stationary problem

Solution of the stationary problem of the flow around a circular cylinder has been obtained by the method of multipole expansions by Li et al. [11]. Here we present only the main results of this solution that are required further for the study of the radiation problem in the next section 4. According to Ref. [11], solution of Eq. (10) with the boundary conditions (11)–(14) can be represented in the form:

$$\overline{\varphi} = \mathrm{Re} \sum_{m=1}^{\infty} a^m C_m \left(\frac{e^{-im\theta}}{r^m} - R_m \right), \tag{23}$$

$$\text{where} \quad R_m = \frac{1}{(m-1)!} \int_0^{\infty} k^{m-1} Z(k) e^{k(y-h-ix)}\, dk; \tag{24}$$

the unknown coefficients C_m to be determined.

Using the well-known relation

$$\frac{\mathrm{e}^{-im\theta}}{r^m} = \frac{1}{(m-1)!} \int_0^{\infty} k^{m-1} e^{-k(y+h+ix)}\, dk \quad (y > -h), \tag{25}$$

and taking into account conditions (11), (12) on the upper boundary of the fluid, we obtain a representation for the function $Z(k)$ in the form:

$$Z(k) = -1 - \frac{2\rho U^2 k}{P(k) - \rho U^2 k}, \quad P(k) = Dk^4 - \left(Q + MU^2\right)k^2 + g\rho. \tag{26}$$

To take into account the boundary condition on the surface of the cylinder (14), we use the relationship:

$$e^{k(y+h-ix)} = 1 + \sum_{m=1}^{\infty} \frac{(kr)^m}{m!} e^{-im\theta}. \tag{27}$$

Then, the stationary potential in the vicinity of the cylinder can be presented up to an insignificant constant in the form:

$$\overline{\varphi} = \mathrm{Re} \sum_{m=1}^{\infty} \left[\frac{a^m}{r^m} C_m - \sum_{n=1}^{\infty} \frac{a^n r^m}{m!(n-1)!} I_{n+m-1} C_n \right] e^{-im\theta}, \quad I_N = \int_0^{\infty} k^N Z(k) e^{-2kh}\, dk. \tag{28}$$

To calculate I_N, let us do the following transformation:

$$I_N = -\frac{N!}{(2h)^{N+1}} - 2\rho U^2 \int_0^{\infty} \frac{k^{N+1}}{P(k) - \rho U^2 k} e^{-2kh}\, dk. \tag{29}$$

The denominator in the integrand, which is the fourth-degree polynomial in k, can be represented as:

$$P(k) - \rho U^2 k = D \prod_{n=1}^{4} (k - k_n), \tag{30}$$

where k_n are the roots of the polynomial. Then, we use the following expansion:

$$\frac{k}{P(k) - \rho U^2 k} = \frac{1}{D} \sum_{n=1}^{4} \frac{\alpha_n}{k - k_n}, \tag{31}$$

where the coefficients α_n can be readily calculated from the solution of the corresponding system of linear algebraic equations obtained from the requirement of equality of the numerator in the right- and left-hand sides of Eq. (31).

The polynomial in the left-hand side of Eq. (30) can be presented in the form:

$$P(k) - \rho U^2 k = (\rho + Mk)(c_p^2 - U^2). \tag{32}$$

As was noted in Ref. [21], the equation

$$P(k) - \rho U^2 k = 0 \tag{33}$$

has real positive roots only for $U > U_p \equiv (c_p)_{min}$. The value of the minimum phase velocity of FGW is $U_p = c_p(k_p)$, where k_p is defined as the real positive root of the equation:

$$Dk^4(2Mk/\rho + 3) - Qk^2 - 2gMk - g\rho = 0. \tag{34}$$

According to Eq. (32), all four roots k_n in Eq. (33) are complex if $U < U_p$, whereas when $U > U_p$, there are two real positive roots k_1 and k_2 ($k_1 < k_2$) and two complex roots k_3 and k_4.

Further we will use the recurrent formulae to calculate the integrals arising in Eq. (29) with the help of Eq. (31). Let us denote

$$J_N = \int_0^\infty \frac{k^N e^{-2kh}}{k - k_n} dk. \tag{35}$$

Before going ahead, let us take into account the Sommerfeld radiation condition at the big distances from the cylinder center (in the far-field zone). This condition presumes that there are only outgoing waves generated by the moving cylinder, i.e., a wave with the wavenumber $k_1(k_2)$ propagates co-current (counter-current), since its phase velocity is greater (less) than the group velocity. Then, for the real roots $k_{1,2}$, we obtain:

$$J_N = \tilde{J}_N - i\pi\chi_n k_n^N e^{-2k_n h}, \quad \text{where} \quad \tilde{J}_N = PV\int_0^\infty \frac{k^N e^{-2kh}}{k - k_n} dk. \tag{36}$$

Here $\chi_n = (-1)^n \quad (n = 1, 2)$, and the symbols PV stands for the principal value of the integral. There is a recurrent formula for $\tilde{J}_N$ [1]:

$$\tilde{J}_{N+1}(k_n) = \frac{N!}{(2h)^{N+1}} + k_n \tilde{J}_N(k_n), \quad \tilde{J}_0(k_n) = -e^{-2k_n h}\mathrm{Ei}(2k_n h), \tag{37}$$

where $\mathrm{Ei}(x)$ is the exponential integral of a real argument.

For complex roots k_n, Eq. (35) reduces to:

$$J_N(z) = \frac{1}{(2h)^N} G_N(z), \quad z = -2hk_n, \tag{38}$$

where

$$G_{N+1}(z) = N! - zG_N(z) \quad (N \geq 1), \quad G_1(z) = 1 - ze^z \mathrm{E}_1(z), \tag{39}$$

and E_1 is the exponential integral of a complex argument [1]. Therefore, the integral term in Eq. (29) can be presented as:

$$\int_0^\infty \frac{k^{N+1}\exp(-2kh)}{P(k) - \rho U^2 k} dk = \frac{1}{D}\sum_{n=1}^{4} \alpha_n J_N(k_n). \tag{40}$$

Differentiating Eq. (28) with respect to r, using the boundary condition (14) with the relations (20), as well as the orthogonality of trigonometric functions, we obtain a system of linear algebraic equations for determining the coefficients C_m in Eq. (23):

$$C_m + \sum_{l=1}^{\infty} \frac{C_l a^{l+m} I_{m+l-1}}{m!(l-1)!} = -ia\delta_{m1}, \tag{41}$$

where δ_{ml} is the Kronecker symbol.

Substituting expression (29) in Eq. (28) for $\overline{\varphi}$ and differentiating with respect to θ, we obtain for $r = a$:

$$\frac{\partial(\overline{\varphi} - x)}{\partial\theta} = -2\mathrm{Re}\left(\sum_{m=1}^{\infty} imC_m e^{-im\theta}\right). \tag{42}$$

After that, the expressions for the stationary forces exerted on the cylinder as follows from Eq. (21) are:

$$F_{s2} - iF_{s1} = \frac{2\pi\rho U^2}{a} \sum_{m=1}^{\infty} m(m+1)C_m^* C_{m+1}. \tag{43}$$

4. Solutions of the radiation problem

Now let us determine the coefficients of the radiation load T_{jk} in Eq. (22). To this end, we need to find the radiation potentials φ_j in formula (8). Let us present the solution for the radiation potentials in the form:

$$\varphi_j = \sum_{m=1}^{\infty} a^m \left[A_{jm}^- \left(\frac{e^{-im\theta}}{r^m} - E_m^-\right) + A_{jm}^+ \left(\frac{e^{im\theta}}{r^m} - E_m^+\right)\right] \; (j = 1, 2). \tag{44}$$

Here the unknown coefficients $A_{jm}^{\pm}$ are to be determined. Taking into account the boundary conditions (16), (17) for the radiation potentials and performing similar manipulations as in Section 3, we obtain the following relations:

$$E_m^{\pm} = \frac{1}{(m-1)!} \int_0^{\infty} k^{m-1} Z^{\pm}(k) e^{k(y-h-ix)}\, dk, \tag{45}$$

where

$$\begin{aligned}
Z^-(k) &= -1 - 2\rho(\Omega + Uk)^2/B^-, && (46)\\
Z^+(k) &= -1 - 2\rho(\Omega - Uk)^2/B^+, && (47)\\
B^- &= (\rho + kM)\left[\omega^2(k) - (\Omega + Uk)^2\right], && (48)\\
B^+ &= (\rho + kM)\left[\omega^2(k) - (\Omega - Uk)^2\right]. && (49)
\end{aligned}$$

Now let us take into account the boundary condition (18) on the surface of the cylinder. Using relation (27), we can write down functions $E_m^{\pm}$ in the vicinity of the cylinder up to an insignificant constant in the form:

$$E_m^{\pm} = \sum_{n=1}^{\infty} \frac{r^n H_{n+m-1}^{\pm}}{n!(m-1)!} e^{\pm in\theta}, \tag{50}$$

where

$$H_N^{\pm} = \int_0^{\infty} k^N Z^{\pm}(k) e^{-2kh}\, dk. \tag{51}$$

Expressions for $H_N^{\pm}$ we present in the form similar to (29):

$$H_N^{\pm} = -\frac{N!}{(2h)^{N+1}} - 2\rho \int_0^{\infty} \frac{k^N}{B^{\pm}} (\Omega \mp Uk)^2 e^{-2kh} \, dk. \tag{52}$$

Functions $B^{\pm}$ in the denominator of the integrand in Eq. (52) are fifth-degree polynomials; by analogy with Eq. (30), they can be written in the form:

$$B^{\pm}(k) = D \prod_{n=1}^{5} (k - k_n^{\pm}). \tag{53}$$

Then, one can use the decomposition:

$$\frac{(\Omega \mp Uk)^2}{B^{\pm}} = \frac{1}{D} \sum_{n=1}^{5} \frac{\beta_n^{\pm}}{k - k_n^{\pm}}, \tag{54}$$

where the coefficients $\beta_n^{\pm}$ are calculated from the solution of the corresponding systems of linear algebraic equations obtained from the requirement of equality of the numerator on the right- and left-hand sides of Eq. (54).

The analysis of the real positive roots $k_n^{\pm}$ we will perform separately for k_n^{+} and k_n^{-}. Below we will briefly present some information about the properties of these roots (for more details see [21]). As follows from Eq. (49) for B^{+}, the roots k_n^{+} must satisfy one of the equations:

$$\omega(k) + \Omega - Uk = 0, \quad \omega(k) - \Omega + Uk = 0. \tag{55}$$

The first equation in (55) defines the stationary points of function Ψ_2 in the notation of paper [21]; it has at most two roots $k_1^{(2)}$ and $k_2^{(2)}$ ($k_1^{(2)} < k_2^{(2)}$) only at certain restrictions on the flow velocity U. The second equation in (55), which determines the stationary points of function Ψ_4 in the notation of [21], always has one positive root, however, it can have two additional roots at certain restrictions on the magnitude of ice compression Q. We denote these roots by $k_1^{(4)} < k_2^{(4)} < k_3^{(4)}$. As follows from the form of function B^{-} in (48), it is easy to see that the roots k_n^{-} must satisfy the equation:

$$\omega(k) - \Omega - Uk = 0. \tag{56}$$

This equation defines the stationary points of function Ψ_3 in the notation of [21].

Equation (56) always has one positive root and possibly, two additional roots at certain restrictions on the frequency of cylinder oscillation Ω and flow velocity U. Let us denote these roots $k_1^{(3)} < k_2^{(3)} < k_3^{(3)}$.

The direction of wave propagation determined by stationary points of functions Ψ_2 and Ψ_3 depends on the sign of the expression $U - c_g(k)$, and for function Ψ_4, on the sign of the expression $U + c_g(k)$, where k should be replaced by the wave numbers corresponding to the stationary points of each function Ψ. Waves with the positives value of these expressions propagate downstream ($x < 0$), whereas waves with the negative values of the expressions propagate upstream ($x > 0$). Therefore, the expressions of $H_N^{\pm}$ in Eq. (52) can be transformed to the form:

$$H_N^{\pm} = -\frac{N!}{(2h)^{N+1}} - \frac{2\rho}{D} \sum_{n=1}^{5} \beta_n^{\pm} J_N(k_n^{\pm}). \tag{57}$$

Here, like in Eq. (36), for the real roots $k_n^{\pm}$, an additional term must be introduced such that $\chi_n = -1$ for waves propagating downstream and $\chi_n = 1$ for waves propagating upstream.

Let us return now to constructing a system of linear algebraic equations for determining the unknown coefficients $A^{\pm}_{jm}$ in Eq. (44). Calculating the second derivatives in the boundary conditions (18), we will use the following relations [27]:

$$\int_0^{2\pi} \frac{\partial^2 \overline{\varphi}}{\partial n \partial x} e^{im\theta}\, d\theta = -\frac{im}{a^2} \int_0^{2\pi} \frac{\partial(\overline{\varphi} - x)}{\partial \theta} e^{im\theta} \sin\theta\, d\theta = \frac{i\pi m}{a^2} P^-_m, \quad (58)$$

$$\int_0^{2\pi} \frac{\partial^2 \overline{\varphi}}{\partial n \partial y} e^{im\theta}\, d\theta = -\frac{im}{a^2} \int_0^{2\pi} \frac{\partial(\overline{\varphi} - x)}{\partial \theta} e^{im\theta} \cos\theta\, d\theta = -\frac{\pi m}{a^2} P^+_m, \quad (59)$$

where $P^{\pm}_m = (m+1)C_{m+1} \pm (m-1)C_{m-1}$.

Differentiating Eq. (44) with respect to r and taking into account Eq. (50) and the boundary conditions (18), we obtain the following systems of linear equations for the determining $A^{\pm}_{jm}$:

$$A^{\pm}_{jm} + \sum_{n=1}^{\infty} \frac{a^{m+n}}{m!(n-1)!} H^{\pm}_{n+m-1} A^{\pm}_{jn} = X^{\pm}_{jm} \quad (j = 1, 2), \quad (60)$$

where

$$X^-_{1m} = (a\Omega\delta_{m1} - iUP^-_m/a)/2, \quad X^+_{1m} = (iUP^{-*}_m/a - a\Omega\delta_{m1})/2, \quad (61)$$

$$X^-_{2m} = (UP^+_m/a - ia\Omega\delta_{m1})/2, \quad X^+_{2m} = (UP^{+*}_m/a - ia\Omega\delta_{m1})/2 \quad (62)$$

The quantities $H^{\pm}_N$ are given in Eq. (57), where the recurrence formulae (37) and (39) are used to calculate $J_N(k^{\pm}_n)$ for the real and complex roots $k^{\pm}_n$, respectively.

On the surface of the cylinder at $r = a$, the values of the radiation potentials are:

$$\varphi_j = \sum_{m=1}^{\infty} \left[\left(2A^-_{jm} - X^-_{jm}\right) e^{-im\theta} + \left(2A^+_{jm} - X^+_{jm}\right) e^{im\theta} \right]. \quad (63)$$

Solving the systems of equations (60), the coefficients of radiation load T_{jk} can be determined. Substituting Eqs. (18) and (63) into (22), we finally obtain:

$$T_{jk} = 2\pi\rho \sum_{m=1}^{\infty} m \left[X^{-*}_{jm} (2A^-_{km} - X^-_{km}) + X^{+*}_{jm} (2A^+_{km} - X^+_{km}) \right]. \quad (64)$$

5. Numerical results

To investigate quantitatively the effect of cylinder oscillation on the ice plate covered an infinitely deep water and hydrodynamic forces exerting on the cylinder, we undertook numerical calculations with the following set of parameters:

$$E = 5 \cdot 10^9 \text{ Pa}, \ \nu = 0.3, \ \rho_1 = 922.5 \text{ kg/m}^3,$$
$$a = 5 \text{ m}, \ h = 10 \text{ m}, \ \rho = 1025 \text{ kg/m}^3, \ g = 9.81 \text{ m/s}^2. \quad (65)$$

Several ice-plate thickness was chosen to study its influence on FGWs and the hydrodynamic characteristics of the cylinder.

Calculations of wave resistance and lift force of a uniform flow around a circular cylinder submerged in a fluid of finite depth cover by ice were studied in Ref. [11]. Figure 6 of this work shows the dependence of the stationary forces on the current velocity for different fluid depths and, in particular, for an infinitely deep fluid. The following dimensionless values of hydrodynamic forces were used:

$$(\overline{F}_{s1}, \overline{F}_{s2}) = (F_{s1}, F_{s2}) / \left(\pi\rho\, g\, a^2\right). \quad (66)$$

Note that in the cited paper [11], the calculations were performed for the case when the ice plate is not compressed ($Q = 0$), and its inertia is neglected ($M = 0$); the thickness of the ice plate was chosen to be $h_1 = 1$ m, and the gravity constant was set to be $g = 9.8$ m/s^2. Other parameters were the same as in Eq. (65). In Figure 2 we present a comparison of the results obtained in Ref. [11] (solid black curve) with our calculations (red dots for $M = 0$ and blue lines for $M = \rho_1 h_1 = 922.5$ kg/m^2). As one can see, the the results of these studies agrees very well for the same sets of parameters. The influence of the inertial parameter M is small and can be neglected in most cases. The dimensionless value of the minimum phase velocity of the FGW $U_p/\sqrt{gh} = 1.6012$ for M = 0 and $U_p/\sqrt{gh} = 1.5648$ for $M = 922.5$ kg/m^2. The effect of ice thickness h_1 on the characteristics of stationary hydrodynamic loads was studied in detail by Li et al. [11].

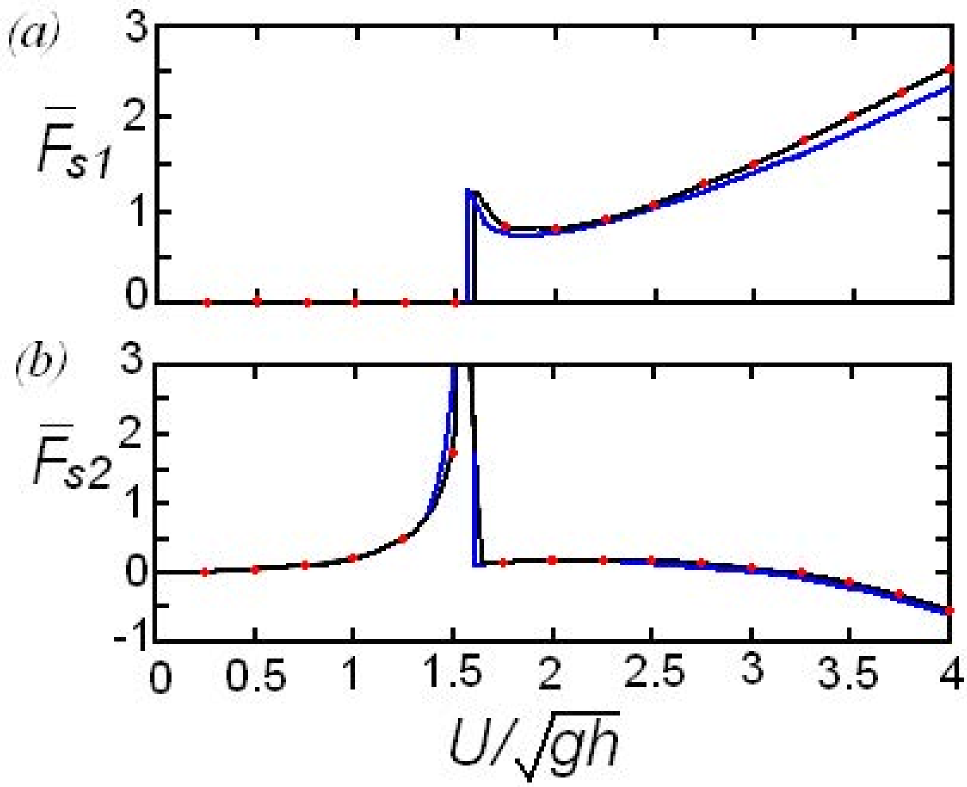

Figure 2. (Color online.) Wave resistance (a) and lift force (b). Solid black lines correspond to the results shown in Figure 6 of Ref. [11] for the infinitely deep fluid; red dots are the results of this work for $M = 0$; blue lines are the results of this work for $M = 922.5$ kg/m^2.

Subsequent calculations presented below were performed for the ice thickness $h_1 = 0.5$ m and different values of the compression parameter $\widetilde{Q} = Q/\sqrt{\rho g D}$. The following dimensionless parameters will be used below:

$$F = \frac{U}{\sqrt{g\,a}}, \ \sigma = \Omega\sqrt{\frac{a}{g}}. \tag{67}$$

For the used parameters the critical dimensionless compression parameter, above which the anomalous dispersion of FGW occurs, is $\widetilde{Q}_0 = 1.4772$. When the numerical calculations were performed, the infinite sums in Eqs. (23) and (44) were replaced by finite sums which contained only the first $N = 8$ terms. A further increase of N does not change the value of the first five significant figures of the hydrodynamic loads. Figure 3 shows the dependence of stationary hydrodynamic forces (43) for $\widetilde{Q} = 0, 1.2, 1.8, 1.95$. The dimensionless values of the critical Froude numbers $F_p \equiv U_p/\sqrt{g\,a}$ for the used values of $\widetilde{Q}$ are given in Table 1.

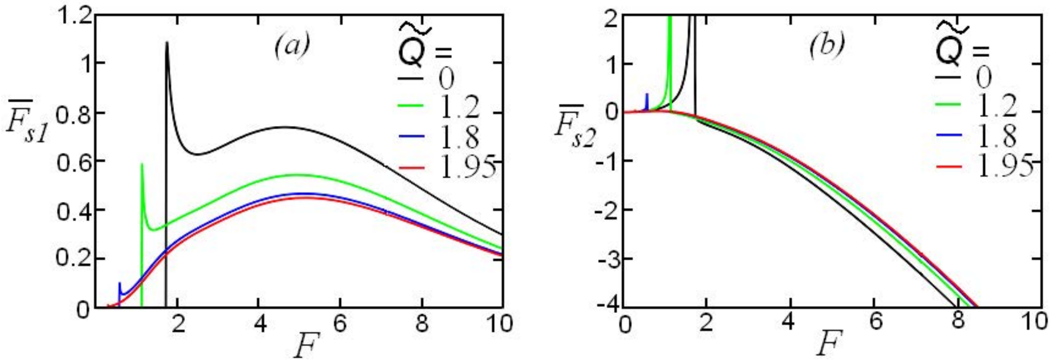

Figure 3. (Color online.) The wave resistance (a) and lift force (b) as functions of the Froude number F for different values of the compression parameter $\widetilde{Q} = 0, 1.2, 1.8, 1.95$.

Table 1. Dependences of the parameters F_p, F_g and σ^* on the normalised compression parameter $\widetilde{Q}$.

$\widetilde{Q}$	F_p	F_g	σ^*
0	1.7124	1.1225	0.2226
1.2	1.1231	0.3311	0.3691
1.8	0.5715	-0.6325	0.6285
1.95	0.2870	-1.2972	0.8650

According to the kinematic properties of FGWs, the excitation of wave motion can occur only for $F > F_p$ in the so-called super-critical regime. Therefore, the wave resistance is identically zero if $F < F_p$ (in the sub-critical regime). When the compression parameter $\widetilde{Q}$ is relatively small, the wave resistance $\overline{F}_{s1}$ sharply increases from zero to some finite value when the Froude number increases and passes through the critical value F_p. Then, when the Froude number further increases, the wave resistance smoothly but non-monotonically decreases. The lift force $\overline{F}_{s2}$ in the sub-critical regime is positive and increases sharply when F approaches F_p; then it sharply decreases when $F > F_p$ and becomes negative. When the compression parameter increases, the jumps of wave resistance and lift force decreases in the vicinity of the critical value F_p. For big Froude numbers, the effect of compression of the ice cover on the wave resistance decreases (see left panel in Figure 3a).

To determine the hydrodynamic loads for the radiation problem, it is necessary to determine a number of generated waves in the far-field zone at the big distance from the cylinder centre. To this end, it is convenient to construct the (F, σ)-plane and determine regions in this plane where the number of generated waves is different. Examples of such diagrams are given in Ref. [21] for the thickness of ice plate $h_1 = 1$ m.

Figure 4 shows the configurations of the regions G_j $(j = 1, ..., 6)$ with the different number of generated waves for the thickness of the ice cover $h_1 = 0.5$ m and several values of the compression parameter $\widetilde{Q} = 0, 1.2, 1.8, 1.95$. In the case of normal dispersion, the (F, σ)-plane is divided into four regions G_j $(j = 1, 2, 3, 4)$ (see Figure 4 (a, b)), whereas in the case of the anomalous dispersion – into six regions (see Figure 4 (c, d)). Small vertical arrows on the horizontal axis show the values of σ^*, and small horizontal arrows on the vertical axis show the values $|F_g|$ (see 1) where $F_g = U_g/\sqrt{ag}$, $\sigma^* \equiv \sqrt{a/g}[\omega(k_g) - U_g k_g]$, and k_g is such that the group velocity of FGWs, c_g in Eq. (7), has a minimum U_g at $k = k_g$.

Table 2 shows the number of waves in the far-field zone and their direction of propagation for each region shown in Figure 4 ($x < 0$ pertains to the downstream propagating waves; $x > 0$ – to the upstream propagating waves).

The values of radiation loads (the added mass and damping coefficients) calculated by using Eqs. (22) and (64) for the Froude number $F = 0.5$ and various values of the compression parameter Q are shown in Figs. 5 (for μ_{ij}) and 6 (for λ_{ij}). The dimensionless values of these quantities are defined as follows:

$$\overline{\mu}_{ij} = \frac{\mu_{ij}}{\rho\, a^2}, \quad \overline{\lambda}_{ij} = \frac{\Omega \lambda_{ij}}{\rho\, g\, a}, \quad (i, j) = 1, 2. \tag{68}$$

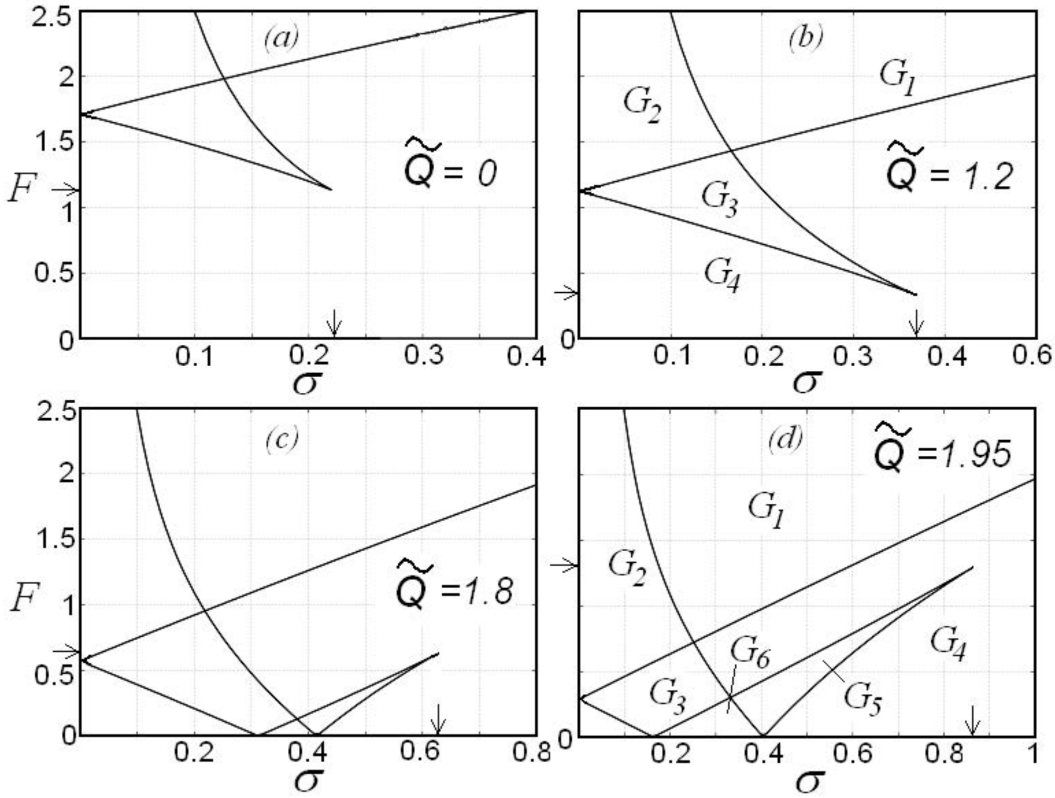

Figure 4. Configuration of the domains G_j $(j = 1, ..., 6)$ for different values of the compression parameter $\widetilde{Q} = 0$ (panel a), 1.2 (panel b), 1.8 (panel c), 1.95 (panel d). The thickness of the ice plate was $h_1 = 0.5$ m.

Table 2. The number of waves in the far-field zone.

G_j	$k_2^{(1)}$	$k_2^{(2)}$	$k_3^{(1)}$	$k_3^{(2)}$	$k_3^{(3)}$	$k_4^{(1)}$	$k_4^{(2)}$	$k_4^{(3)}$
G_1	$x < 0$	$x > 0$	$x > 0$	-	-	$x < 0$	-	-
G_2	$x < 0$	$x > 0$	$x > 0$	$x < 0$	$x > 0$	$x < 0$	-	-
G_3	-	-	$x > 0$	$x < 0$	$x > 0$	$x < 0$	-	-
G_4	-	-	$x > 0$	-	-	$x < 0$	-	-
G_5	-	-	$x > 0$	-	-	$x < 0$	$x > 0$	$x < 0$
G_6	-	-	$x > 0$	$x < 0$	$x > 0$	$x < 0$	$x > 0$	$x < 0$

As can be seen from Figs. 5 and 6, the hydrodynamic loads smoothly depend on the oscillation frequency only when $\widetilde{Q} = 0$ since in this case, for all frequencies and fixed Froude number $F = 0.5$, the boundaries of the regions G_j are not crossed (see Figure 4a). In all other investigated cases of the compression parameter $\widetilde{Q} = 1.2, 1.8, 1.95$, there are sharp changes in the values of the hydrodynamic loads in the vicinity of the

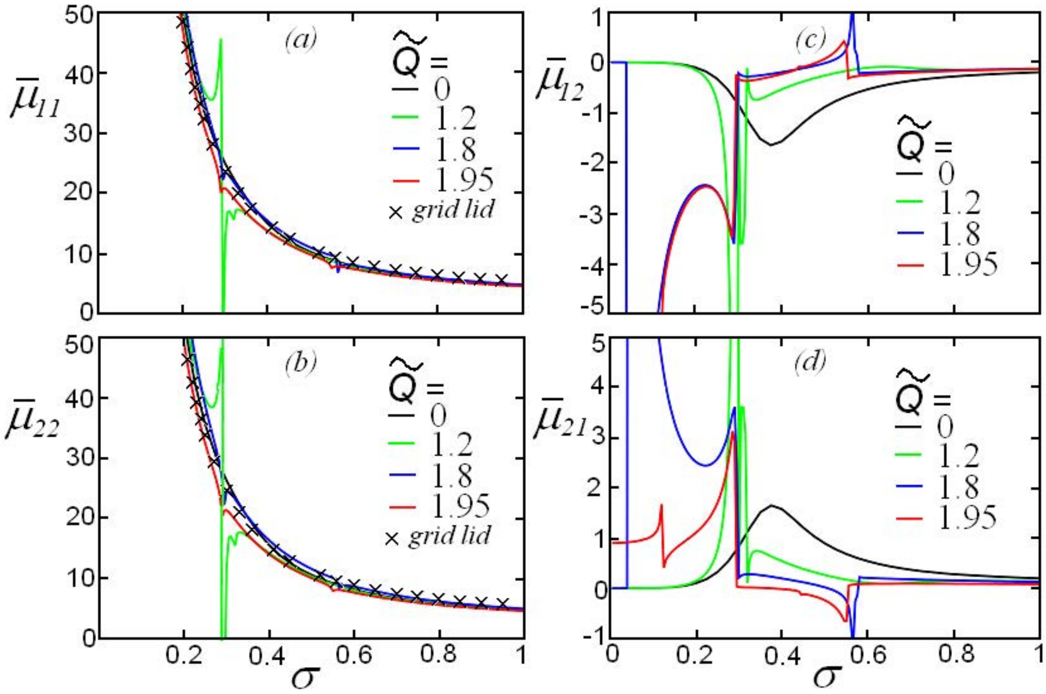

Figure 5. (Color online.) Dependence of the added mass coefficients: $\overline{\mu}_{ij}$ $(i,j) = 1,2$ on the dimensionless frequency of cylinder oscillation for $\widetilde{Q} = 0, 1.2, 1.8, 1.95$ and fixed Froude number $F = 0.5$. Crosses show the values of $\overline{\mu}_{11}$ and $\overline{\mu}_{22}$ for the fluid covered by a rigid lid.

frequencies corresponding to the boundaries of the regions G_j. The hydrodynamic loads in the vicinity of these frequencies can significantly exceed the corresponding values for the uncompressed ice when $\widetilde{Q} = 0$. For a given Froude number $F = 0.5$, the diagonal coefficients of the added mass matrix in the cases of uncompressed ice and rigid cover practically coincide, they are indistinguishable in panels (a) and (b) of Figure 5.

Similar dependences of the hydrodynamic loads on the oscillation frequency are shown in Figs. 7 and 8 for the Froude number $F = 1$. In panel (a) and (b) of Figure 7, the values of the added mass coefficients are practically indistinguishable for $\widetilde{Q} = 1.8$ and $\widetilde{Q} = 1.95$. When the Froude number increases, the frequency dependences of hydrodynamic loads notable change even in the case of $\widetilde{Q} = 0$. In the vicinity of the frequency $\sigma = \sigma_*$, there is a sharp change in the coefficients, since the considered value of the Froude number $F = 1$ is close to the value of F_g for $\widetilde{Q} = 0$ (see Table 1).

As well-known, at the superposition of the slow translational and oscillatory motion of a circular cylinder in a water with the free surface, the Timman–Newman symmetry conditions are satisfied [28]:

$$\mu_{12} = -\mu_{21}, \quad \lambda_{12} = -\lambda_{21}. \tag{69}$$

In the considered problem of cylinder motion under a compressed ice cover, the fulfillment of these conditions is observed for $F = 0.5$ and $\widetilde{Q} = 0, 1.2, 1.8$, as well as for $F = 1$ and $\widetilde{Q} = 0, 1.2$.

An interesting feature of the considered problem is the possibility of appearance of negative values for the diagonal damping coefficients $\overline{\lambda}_{11}$ and $\overline{\lambda}_{22}$ for the Froude numbers corresponding to the decrease in the wave resistance with increasing cylinder velocity (the so-called falling wave resistance section). According to Figure 3(a), this phenomenon of wave resistance is observed when $F > 5$ for all considered compression parameters. For the illustration, we show in Figure 9 the diagonal damping coefficients for $F = 7$.

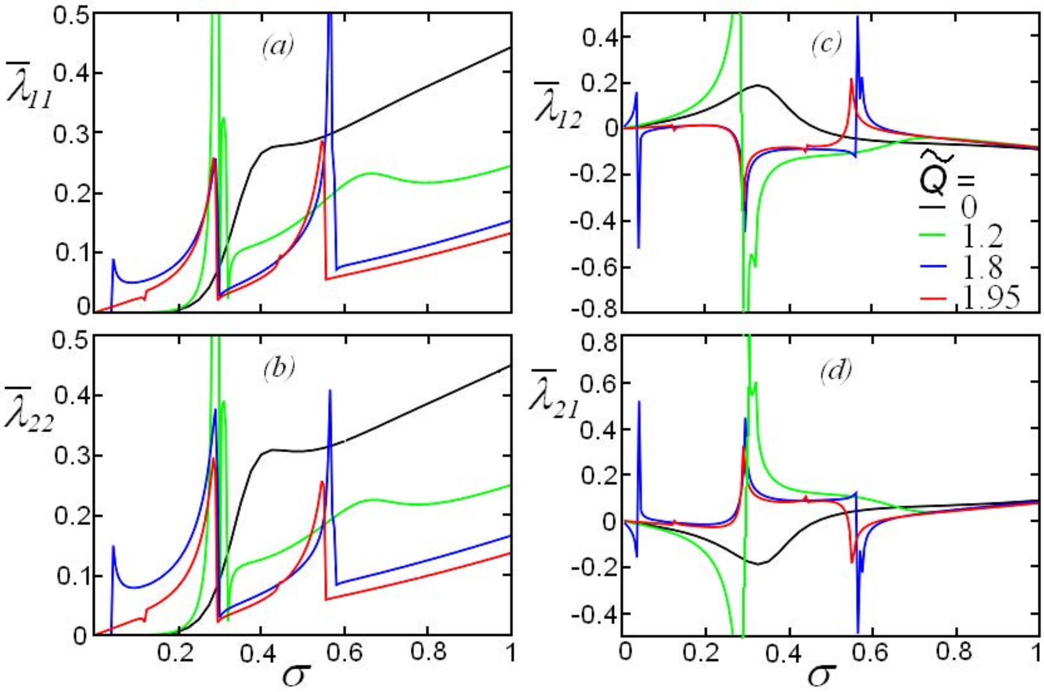

Figure 6. (Color online.) Dependence of the damping coefficients: $\overline{\lambda}_{ij}$ $(i,j) = 1,2$ on the dimensionless frequency of cylinder oscillation for $\widetilde{Q} = 0, 1.2, 1.8, 1.95$ and fixed Froude number $F = 0.5$.

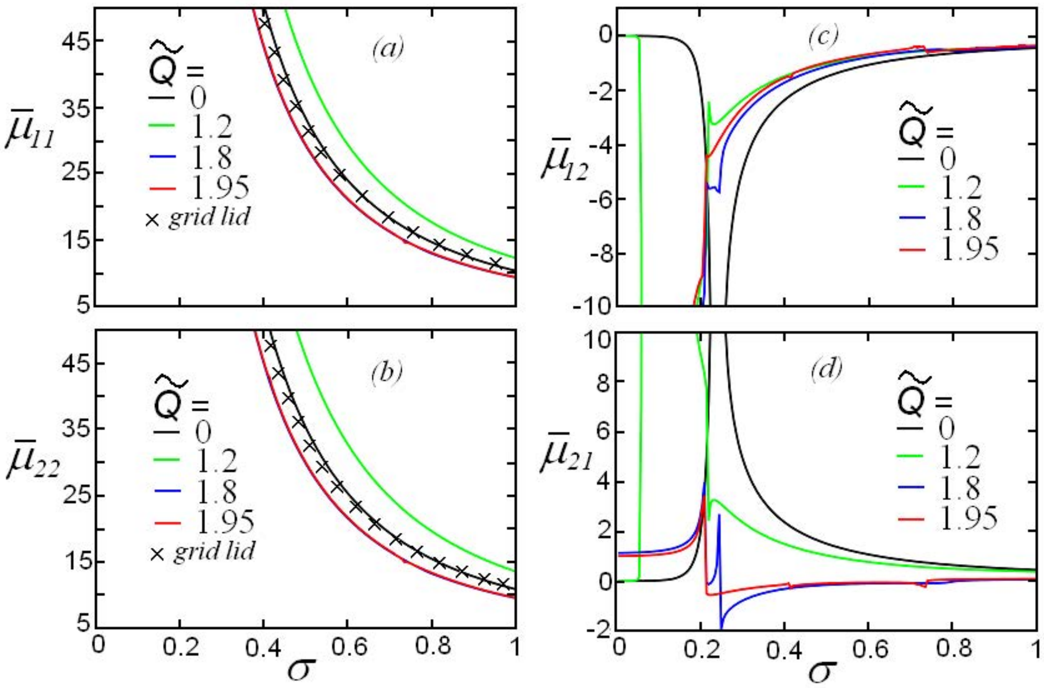

Figure 7. (Color online.) Similar to what is shown in Figure 5 but for $F = 1$.

The negative damping coefficients, apparently, was obtained for a first time by Newman [12] when he calculated the hydrodynamic loads exerting on an ellipsoid uniformly moving under the free surface of a homogeneous fluid and simultaneously oscillating along one of six degrees of freedom. It was noted that this phenomenon occurs only at high speeds of motion. Usually, the wave resistance increases when the speed increases at relatively low speeds, but then, when the speed becomes high enough, the wave resistance decreases when the speed of a body further increases. In this range

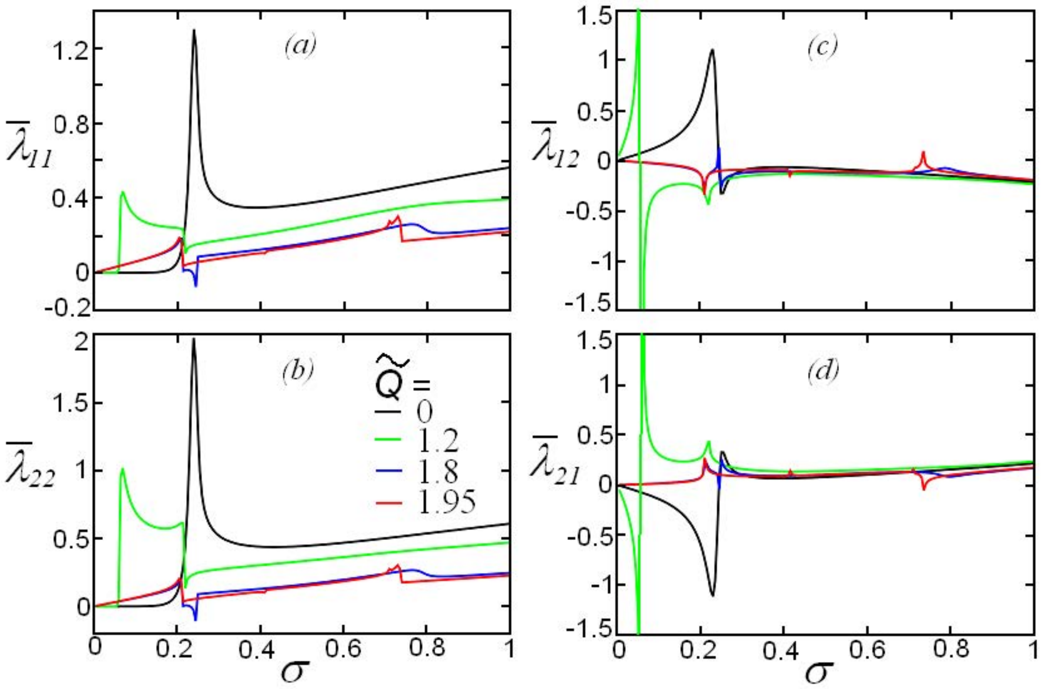

Figure 8. (Color online.) Similar to what is shown in Figure 6 but for $F = 1$.

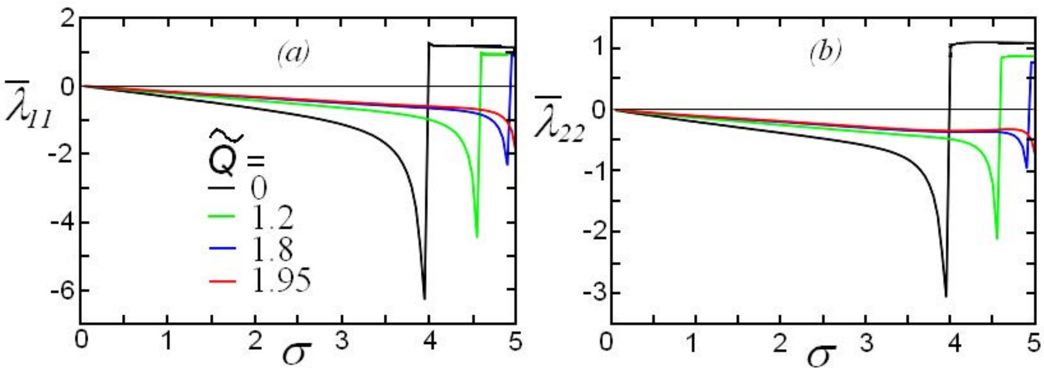

Figure 9. (Color online.) The diagonal damping coefficients $\overline{\lambda}_{11}$ (panel a) and $\overline{\lambda}_{22}$ (panel b) for $\widetilde{Q} = 0, 1.2, 1.8, 1.95$ and Froude number $F = 7$.

of the velocities, the motion of an oscillating body in a fluid can be accompanied by the radiation instability when the amplitude of oscillations increases with time due to the pumping of energy into the oscillatory mode from the kinetic energy of the translational motion. The physical analysis of this phenomenon was carried out in Ref. [7] with the example of the motion of a small-radius sphere in a two-layer fluid. The complete solution of the linear radiation problem for a circular cylinder in a uniform flow of an infinite two-layer fluid made it possible to determine the dependences of hydrodynamic loads on the speed of the body and frequency of oscillations. Using these results, a system of ordinary differential equations was derived to describe the motion of a cylinder with two degrees of freedom, and the possibility of onset of non-decaying oscillations of the body was shown [23,24].

As the particular case of the radiation problem let us consider radiation caused by the submerged oscillating cylinder without a translational speed, $U = 0$. In this case, the solution presented above significantly simplifies. In the expression for the radiation force T_{jk} in the formula (22) only the diagonal terms are non-zero, $T_{11} = T_{22} \neq 0$. The detailed solution to this problem is presented in Ref. [21]. The effect of ice compression on the hydrodynamic loads is illustrated by Figure 10. In this figure one can see the frequency dependences of the added mass $\overline{\mu} = \mu_{jj}/(\pi\rho\, a^2)$ (left panel) and damping coefficient $\overline{\lambda} = \lambda_{jj}/(\pi\rho\, a^2\Omega)$ (right panel) for a few values of the parameter $\widetilde{Q} = 1.2, 1.4, 1.8$. In the first two cases the normal dispersion of FGWs takes place, whereas in the latter case the dispersion is anomalous so that FGWs with the negative group velocities appear in the range of dimensionless frequencies $0.312 < \sigma < 0.415$. As one can see from this figure, in the presence of ice compression, the extreme values of hydrodynamic loads significantly increase in the vicinity of frequencies where the group velocity of FGWs becomes very small or changes its sign.

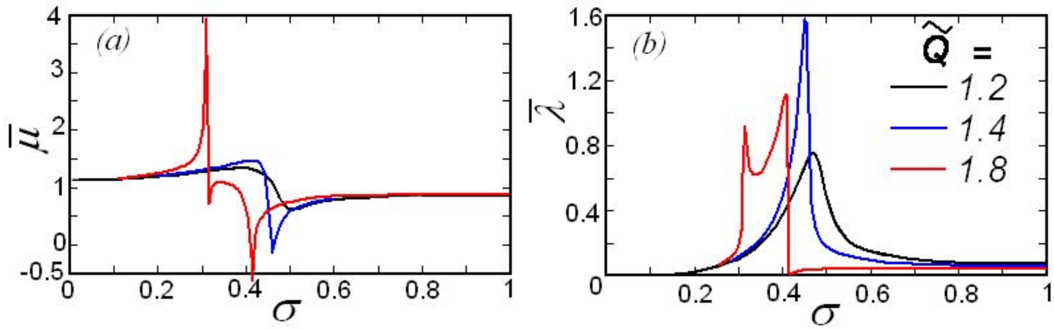

Figure 10. (Color online.) The frequency dependences of the added mass $\overline{\mu}$ (left panel) and damping coefficient $\overline{\lambda}$ (right panel) for a few values of the parameter $\widetilde{Q} = 1.2$, 1.4, 1.8.

6. Conclusions

As was shown in this paper, the ice cover provides a significant influence on the hydrodynamic loads of circular cylinder in the uniform current. Even in the case when there is no mean flow and a cylinder experiences only oscillations the added mass and damping coefficient can significantly differ from those values when there is no ice cover. Moreover, ice compression plays an important role providing increase of hydrodynamic loads within a certain intervals of frequency of cylinder oscillation. The dependences of the added mass and damping coefficient on frequency has a resonant character (see Figures 5–10) with the extremal values in the vicinity of such frequencies where the group velocity of FGWs becomes very small or changes its sign. Sch a situation when the group velocity is opposite to the phase velocity in a certain range of wavenumbers and the anomalous dispersion of FGWs occurs is realisable when the rate of ice compression is high enough.

We have investigate also the dependences of hydrodynamic loads (the added mass, damping coefficients, wave resistance, and lift force) exerting on the cylinder uniformly moving and oscillating. It has been shown that there is such a regime of motion when negative values for the damping coefficients occur. Such a phenomenon is well-known in the case of a body moving with oscillations beneath a free surface [7,12]. Here we have demonstrated that a similar phenomenon can occur in the ocean covered by compressed ice. We have investigated the dependence of the effect on the rate of compression. As one can see from Figure 9, the maximal negative value of the damping coefficients decreases with the increase of ice compression and shifts toward the high frequencies.

The results obtained can be useful in the design of underwater pipelines and other engineering constructions in the marine zones covered by ice. Tidal flows and other currents can produce significant loads on the constructions and lead to the development of instabilities with big-amplitude oscillations. We considered here rather idealised model neglecting viscosity and nonlinear effects. The influence of these factors deserves further study.

Author Contributions: Conceptualization, Y.S. and I.S.; methodology, Y.S. and I.S.; software, I.S.; validation, I.S.; formal analysis, Y.S. and I.S.; investigation, Y.S. and I.S.; resources, I.S.; writing—

original draft preparation, I.S.; writing—review and editing, Y.S. and I.S.; visualization, I.S. All authors have read and agreed to the published version of the manuscript.

Funding: Y.S. acknowledges the funding of this study provided by the grant SPARC/2018-2019/P751/SL through the Scheme for Promotion of Academic and Research Collaboration of the Ministry of Human Resource Development, Government of India, by the grant No FSWE-2020-0007 through the State task program in the sphere of scientific activity of the Ministry of Science and Higher Education of the Russian Federation, and the grant number NSH-2685.2018.5 provided by the President of Russian Federation for the State support of leading Scientific Schools of the Russian Federation.

Conflicts of Interest: The authors declare no conflict of interest.

Abbreviations

The following abbreviation is used in this manuscript:

FGW flexural-gravity wave

References

1. Abramowitz, M.: Stegun, I. A. *Handbook of Mathematical Functions*; National Bureau of Standards, 1964.
2. Bukatov, A. E. *Waves in the Sea With a Floating Ice Cover*; Marine Hydrophy. Inst, Sebastopol, 2017, in Russian: http://mhi-ras.ru/news/news_201802151133.html.
3. Das, S.; Kar, P.; Sahoo, T.; Meylan, M. H. Flexural-gravity wave motion in the presence of shear current: wave blocking and negative energy waves. *Phys. Fluids* **2018**, *30* 106606 (2018).
4. Das, S.; Sahoo, T.; Meylan, M. H. Dynamics of flexural gravity waves: from sea ice to Hawking radiation and analogue gravity. *Proc. R. Soc. A.* **2018**, *474*, 2017223 (2018).
5. Das, S.; Sahoo, T.; Meylan, M. H. Flexural-gravity wave dynamics in two-layer fluid: blocking and dead water analogue. *J. Fluid Mech.* **2018**, *854*, 121–145.
6. Davys, J. W.; Hosking, R. J.; Sneyd, A. D. Waves due to a steadily moving source on a floating ice plate. *J. Fluid Mech.* **1967**, *180*, 297–318.
7. Gaponov-Grekhov, A. V.; Dolina, I. S.; Ostrovsky, L. A. The anomalous Doppler effect and radiative instability of the motion of oscillators in hydrodynamics. *Sov. Phys. Docl.* **1983**, *28(2)*, 117–119.
8. Il'ichev, A. T.; Savin, A. A.; Savin, A. S. Formation of wave on an ice-sheet above the dipole, moving in a fluid. *Doklady Phys.* **2012**, *57*, 202–205.
9. Kheisin, D. Ye. *Dynamics of Floating Ice Cover*; Gidrometeoizdat, Leningrad, 1967, in Russian; Technical English Translation in: FSTC-HT-23-485-69, U.S. Army Foreign Science and Technology Center.
10. Krasil'nikov, V. V. On excitation of flexural-gravity waves. *Akust. Zhurnal (in Russian)* **1962**, *8*, 133–136.
11. Li, Z. F.; Wu, G. X.; Shi, Y. Y. Interaction of uniform current with a circular cylinder submerged below an ice sheet. *Appl. Ocean Res.* **2019**, *86*, 310–319.
12. Newman, J. N. The damping of an oscillating ellipsoid near a free surface. *J. Ship Res.* **1961**, *5(3)*, 44–58.
13. J. N. Newman, *Marine hydrodynamics* (Cambridge, Mass.; London, 1985).
14. Pavelyeva, E. B.; Savin, A. S. Establishment of waves generated by a pulsating source in a finite-depth fluid. *Fluid Dyn.* **2018**, *53*, 461–470.
15. Sahoo, T. *Mathematical Techniques for Wave Interaction with Flexible Structures*; CRC Press, 2012.
16. Savin, A. A.; Savin, A. S. Ice cover perturbation by a dipole in motion within a liquid. *Fluid Dyn.* **2012**, *47*, 139–146.
17. Savin, A. A.; Savin, A. S. Waves generated on an ice cover by a source pulsating in fluid. *Fluid Dyn.* **2013**, *48*, 303–309.
18. Savin, A. A.; Savin, A. S. Three-dimensional problem of disturbing an ice cover by a dipole moving in fluid. *Fluid Dyn.* **2015**, *50*, 613–620.
19. Schulkes, R. M. S. M.; Hosking, R. J.; Sneyd, A. D. Waves due to a steadily moving source on a floating ice plate. Pt. 2. *J. Fluid Mech.* **1987**, *180*, 297–318.
20. Squire, V. A. Ocean wave interactions with sea ice: A reappraisal. *Annu. Rev. Fluid Mech.* **2020**, *52*, 37–60.

21. Stepanyants, Y.; Sturova, I. Waves on a compressed floating ice plate caused by motion of a dipole in water. *J. Fluid Mech.* **2021**, *907*, A7.
22. Sturova, I. V. Planar problem of hydrodynamic shaking of a submerged body in the presence of motion in a two-layer. *J. Appl. Mech. Technical Phys.* **1994**, *35(5)*, 670–679.
23. Sturova, I. V. Radiation instability of a circular cylinder in a uniform flow of a two-layer fluid. *J. Appl. Math. Mechs.* **1997**, *61(6)*, 957–965.
24. I. Sturova, Radiative instability of the circular cylinder in a uniform current of a two-layer fluid, The 22-nd Symposium on Naval Hydrodynamics. Washington, USA, 1998, preprints, pp. 1–9.
25. Sturova, I. V. Unsteady three-dimensional sources in deep water with an elastic cover and their applications. *J. Fluid Mech.* **2013**, *730*, 392–418.
26. Wu, G. X. Hydrodynamic forces on a submerged cylinder advancing in water waves of finite depth. *J. Fluid Mech.* **1991**, *224*, 645–659.
27. Wu, G. X. Radiation and diffraction of water waves by a submerged circular cylinder at forward speed. *J. Hydrodyn. Ser. B.* **1993**, *5(4)*, 85–96.
28. Wu, G. X.; Eatock Taylor, R. Reciprocity relations for the hydrodynamic coefficients of bodies with forward speed. *Intl. Shipbuild. Prigr.* **1988**, *35(402)*, 145–153.

Short Biography of Authors

Yury Stepanyants graduated in 1973 with the HD of MSc Diploma (Russia) and started to work as the Engineer with the Research R Then, he proceeded his career with the Institute of Applied Phys Sciences (Nizhny Novgorod) taking successively the positions of Juni Scientist from 1977 to 1997. In 1983 Yury obtained a PhD in Physi he obtained a degree of Doctor of Sciences in Geophysics. After in Yury worked for 12 years as the Senior Research Scientist with the Technology Organisation in Sydney. Since July 2009 he holds a p University of Southern Queensland in Toowoomba, Australia. Yur journal papers, 3 books, several review papers and has obtained interests are in: Hydrodynamics and geophysical fluid mechanics; and waves; Exact and asymptotic solutions of nonlinear equation computational physics.

Izolda Sturova graduated from Novosibirsk State University i Institute of Hydrodynamics where she works until now. She Researcher, Junior Scientist (since 1967), Senior Scientist (since (since 1988), Head of a Sector (since 1991), and Chief Scientist (fr she obtained a PhD degree in Fluid Mechanics, and in 1995 the de Mechanics. Izolda is the author of over 100 scientific publication research interests are: surface, internal and flexural-gravity waves floating platforms.